

Stability Issues and Structure-Sensitive Magnetic Properties of Nanofluid Ferromagnetic Graphite

N. S. Souza¹, S. Sergeenkov^{1,*}, A. D. Rodrigues², C. A. Cardoso¹, H. Pardo³, R. Faccio³, A. W. Mombrú³, J. C. Galzerani², O. F. de Lima⁴, and F. M. Araújo-Moreira¹

¹Materials and Devices Group, Department of Physics, Universidade Federal de São Carlos, 13565-905 São Carlos, SP, Brazil

²Raman Spectroscopy in Nanostructured Materials, Department of Physics, Universidade Federal de São Carlos, 13565-905 São Carlos, SP, Brazil

³Facultad de Química, Crystallography, Solid State and Materials Laboratory (Cryssmat-Lab), DEQUIFIM, Universidad de la República, P.O. Box 1157, CP 11800, Montevideo, Uruguay

⁴Instituto de Física “Gleb Wataghin,” UNICAMP, 13083-970 Campinas, SP, Brazil

We present our recent results on the application oriented properties of nanofluid ferromagnetic graphite (NFMG) with an average particle size of the order of 10 nm. The obtained high values of the Zeta potential (reaching 40.5 mV, 41.7 mV and 42.3 mV for pH levels equal to 6, 7 and 8, respectively) indicate a good stability of the dispersed solution. A rather strong reactivity between nanofluid ingredients and the cationic surfactant was evidenced by using the diffuse reflectance infrared Fourier transform (DRIFT) spectroscopy. The measured hysteresis curves confirm a robust ferromagnetic behavior of NFMG even at room temperatures. The observed structure sensitive temperature oscillations of magnetization are interpreted as a strongly coherent thermomagnetic response of the nanofluid important for its biological applications.

KEYWORDS: Nanofluid, Ferromagnetic Graphite, Magnetic Hysteresis, Magnetization, Zeta Potential, Raman and DRIFT Spectroscopy.

1. INTRODUCTION

The suspended colloids of nano sized iron oxide particles (Fe_3O_4 or $\gamma\text{-Fe}_2\text{O}_3$) are probably the most recognizable magnetically controllable nanofluids (simultaneously exhibiting both *fluid* and *magnetic* properties). At the same time, the important for applications biocompatible ferrofluids normally use water as a vehicle. In order to prevent agglomeration, the magnetic nanoparticles have to be stabilized by ionic interaction using some kind of bioagent (like, e.g., fatty, aspartic and glutamic acids or peptides). Alternatively, the co-precipitation of ferrous/ferric ions can be obtained in the presence of the appropriate biopolymer (such as polyvinyl alcohol or polyethylen glycol). Several clinically important enzymes and proteins (including, among others, bovine serum albumin, streptokinase, chymotrypsin, and glucose oxidase) have been immobilized based on this method. Recently,

quite a substantial progress has been made in developing suspended colloids of nano sized magnetic particles, including carbon, graphite and graphene based nanofluids and biocompatible ferrofluids (see, e.g., Refs. [1–19] and further references therein). In particular, Parkansky et al.¹⁴ successfully separated magnetic carbon particles (including chains of nanospheres with diameters from 30 to 50 nm, and nanorods with lengths from 50 to 250 nm and diameters from 20 to 30 nm) in the obtained solutions by means of the bio-ferrography technique. At the same time, Widenkvist et al.¹⁷ suggested a new method to produce suspensions of graphene sheets (graphite flakes) by combining solution-based bromine intercalation and mild sonochemical exfoliation. Since carbon is the most abundant chemical element in living beings (including humans), its magnetic modifications, undoubtedly, open new and extraordinary possibilities for applications in medicine and biology (especially given its unique biological and physiological compatibilities). Several of these applications are closely related to bionanotechnology, which is at the edge of the fast developing field of nanotechnology. Some of the goals in this field include relevant improvements in such important areas as drug delivery, medical

*Author to whom correspondence should be addressed.

Email: sergei@df.ufscar.br

Received: 17 September 2012

Accepted: 26 September 2012

diagnosis, therapy, molecular biology and bioengineering. The nanosized systems become especially interesting and important when they are constructed via biocompatible magnetic nanoparticles.^{20–23}

Focusing on the possible biological applications of ferromagnetic graphite, we have developed a process for its obtention in the form of a nanofluid ferromagnetic graphite (NFMG). In the present paper, we present our latest results on the structure, stability and some unique magnetic properties of room temperature NFMG.

2. EXPERIMENTAL DETAILS

2.1. Preparation

The chemically modified magnetic graphite (MG) reported here was produced by a vapor phase redox reaction in closed nitrogen atmosphere (N_2 , 1 atm.) with copper oxide using synthetic graphite powder (Fluka, granularity < 0.1 mm). After obtaining the MG,^{24–26} we have prepared the nanofluid suspension (NFMG)²⁷ by dissolving graphite in acetone, adding a Cetyltrimethylammonium bromide (CTAB) cationic surfactant, and bringing it to an ultra sonic edge. The resulting homogeneous solution was separated in a centrifuge at 6000 rpm. After five consecutive washes with acetone (to remove an excessive surfactant), deionized water was added and the solid sample was brought back to an ultra sonic edge for 1 min. The above procedure provided the necessary homogeneity and stability of the obtained solution. The adsorption of active agents on the surface of the graphite results from the favorable interaction between the surface and species of the solid adsorbents. Various interactions (such as electrostatic attraction, covalent binding, hydrogen binding, non-polar interactions and lateral interactions between adsorbed species) can contribute to the adsorption processes, facilitating the aqueous suspension of graphite.

2.2. Characterization

The structural characterization of NFMG was performed by transmission electron microscopy (TEM) using Philips CM-120 microscope. TEM analysis (see Fig. 1) reveals a flake like morphology of NFMG. Relating the size of the scale in Figure 1 with the size of the particle in the nanofluid, the latter is estimated to be of the order of $l = 10$ nm. To assess the presence of CTAB molecules on the surface of NFMG, we performed micro Raman analysis with samples of graphite dried in vacuum at 60 °C for 6 hours. As expected, the CTAB functional groups, the hydrophobic (carbonic chain) and hydrophilic (cationic-active agents with positive charge) parts of the surfactant are found to correlate with the band structure of the graphite. Since the hydrophilic part tends to bind with the water molecules, its action results in stabilization of

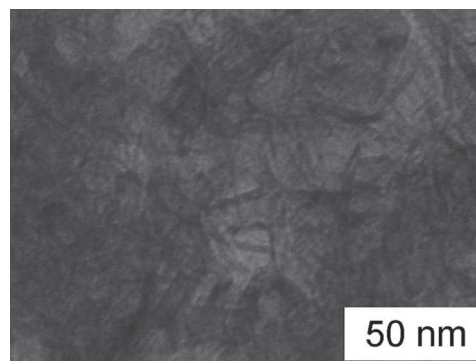


Fig. 1. TEM picture of nanofluid ferromagnetic graphite with resolution of 50 nm, showing a flake-like structure of the aqueous suspension with an average particle size of the order of 10 nm.

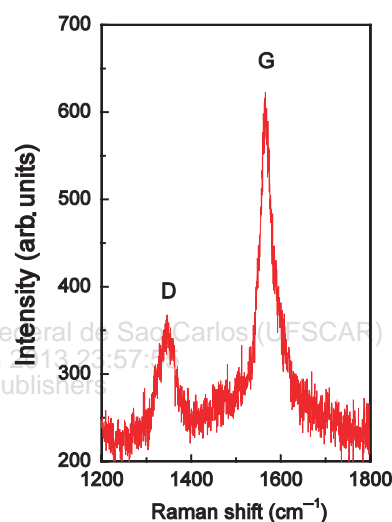


Fig. 2. Raman spectra of the nanofluid ferromagnetic graphite. *G* and *D* peaks are related to the in-plane phonon and the disorder activated modes, respectively.

the nanofluid suspension. As it can be seen in Figure 2, the Raman spectra of the NFMG samples present the traditional phonon-mediated *G*-band (seen also in MG samples) and the disorder activated *D*-band. The relationship between the integral intensity of the *D*-band (I_D) and the *G*-band (I_G) can be used to determine the graphite nanocrystalline size l through a simple equation:²⁸ l (nm) = $(4.36I_G)/I_D$. By applying this idea to the Raman spectra measured in our samples, we have obtained l equal to 11 nm and 10 nm for MG and NFMG, respectively. These values are in good agreement with those determined from the TEM image, shown in Figure 1.

3. RESULTS AND DISCUSSION

3.1. Stability Issues

The important for applications question on stability of NFMG was verified via Zeta potential (ZP) measurements

of the nanoparticles under suspension using Zeta Sizer Nano equipment.²⁹ Recall that ZP indicates the level of the repulsion between particles similarly charged in dispersion and it is directly related to their electrophoretic mobility. If the dispersed phase is formed by small particles, then ZP value will indicate how stable the dispersion is. This means that the higher is the ZP, the more the dispersion will resist aggregation, resulting in a longer period of stability. More specifically,²⁹ ZP values higher than ± 61 mV lead to an excellent stability. Our preliminary results reported earlier³⁰ on ZP measurements for pH level at a fixed value of 7 produced 41.3 mV for NFMG. Some interesting dependencies of ZP on pH level for carbon nanotube (CNT) dispersion have been reported by Xie and Chen³¹ in the context of adjustable thermal conductivity of CNT nanofluids. To test the sensitivity of ZP to pH level in our nanofluids, we measured ZP of NFMG for 3 different values of pH and obtained 40.5 mV, 41.7 mV and 42.3 mV for pH = 6, 7 and 8, respectively. The higher values of ZP in the present nanofluid (even for pH = 7) are achieved by improving the interaction between the graphite particles and the liquid phase. To visualize these improvements, we have performed diffuse reflectance infrared Fourier transform (DRIFT) spectroscopy using a Blücher spectrophotometer. For this characterization, the NFMG sample was dried under vacuum at 60 °C for 6 hours. Notice that the present DRIFT spectrum of NFMG (shown in Fig. 3) significantly deviates from the one³⁰ obtained for previously measured nanofluid (especially, below 2000 cm^{-1}). These spectral changes are attributed to better functionalization of the CTAB molecules on the edges of the nanographite particles in a more stable solution. Since the primary bonds between the carbon atoms in graphite act only in the basal plane, no dangling bonds are generated when the

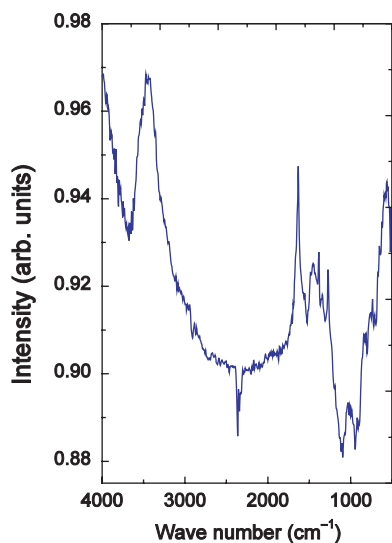


Fig. 3. Diffuse reflectance infrared Fourier transform (DRIFT) spectrum of nanofluid ferromagnetic graphite.

structure is sectioned parallel to the basal plane. As a result, after the breaking of the secondary forces between the basal planes, the graphite lamellas have superficial energy significantly lower than materials in which dangling bonds are generated on surface, as in the case of the oxides.

3.2. Structure-Sensitive Magnetic Properties

First of all, to prove ferromagnetic nature of our NFMG sample, we have analyzed its magnetization as a function of magnetic field (M - H hysteresis curves) at room temperature (see Fig. 4). The measurements were performed with a Quantum Design MPMS-5T SQUID magnetometer. In addition to the fact that the hysteresis does not vanish even at room temperature, we also observe non-zero values for both the remnant magnetization and the coercive magnetic field. That is why we can safely conclude that the nanofluid does not exhibit a conventional superparamagnetic behavior (as, for example, in the case of iron oxides), but instead it follows a verifiable and well defined ferromagnetic pattern (previously confirmed for another similar sample²⁷).

Furthermore, to test the magnetic properties of NFMG samples, we performed the standard zero field cooled (ZFC) and field cooled (FC) measurements using the same magnetometer. Figure 5 presents the temperature dependence of the ZFC magnetization M showing a well-defined Curie temperature around 300 K. Besides, like in our previous measurements (with another sample),³² above 100 K we observe very pronounced temperature oscillations of M which can be attributed to the local variation of the magnetization $M(r)$ defined by the periodic radial distribution function (also known as a pair correlation function) $g(kr)$ as follows³³ $M(r) = M_0 g(kr)$, and assuming that the wave vector k is temperature dependent (see Ref. [32] for detailed discussion). More specifically, we assume that $k(T) \propto M_b(T)/M_b(T_m)$ where $T_m = 100$ K and $M_b(T)$ is the bulk spontaneous magnetization of the single ferromagnetic particle given by the

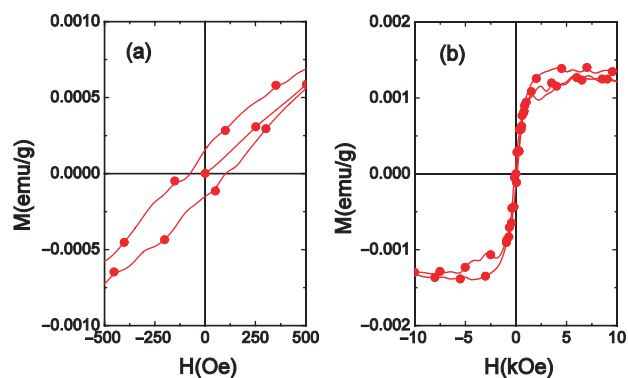


Fig. 4. The room-temperature hysteresis curves of nanofluid ferromagnetic graphite for low (a) and high (b) magnetic fields.

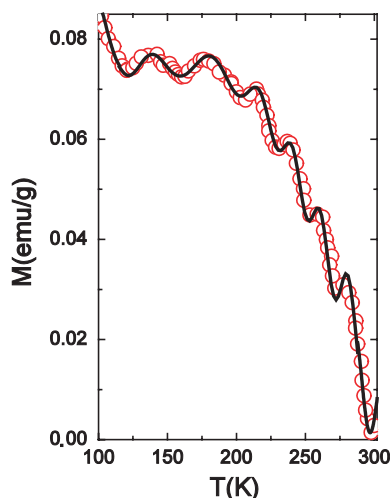


Fig. 5. The structure-sensitive temperature oscillations of the ZFC magnetization observed in nanofluid ferromagnetic graphite.

Curie-Weiss expression (valid below the Curie temperature $T_C = 300$ K)

$$M_b(T) = M_b(0) \tanh \left\{ \sqrt{\left(\frac{T_C}{T}\right)^2 - 1} \right\} \quad (1)$$

As a result, the temperature dependence of the observed magnetization of the magnetic nanofluid can be described as follows^{32,33}

$$M(T) = \left(\frac{1}{L}\right) \int_0^L r^2 dr M_0 g(kr) \quad (2)$$

where $L = Nl$ is an average cluster size with l being a size of the single particle and N the number of particles forming the cluster. The best fits (shown by the solid line in Fig. 5) of the magnetization data using Eqs. (1) and (2) revealed a hard-sphere type pair correlations³³ between graphite particles in the nanofluid with $g(kr) = \sin(kr)/r^2$ and produced $N = L/l = 15$ for the number of particles contributing to the observed oscillating behavior (which is quite close to the number deduced from another sample's data³²).

4. CONCLUSION

We presented our recent results on preparation, characterization, and magnetic properties of a stable dispersed solution of room temperature ferromagnetic graphite which are important for biological applications. The obtained magnetic nanofluid has a flake-like structure of the aqueous suspension with an average particle size of the order of 10 nm. The measured hysteresis curves confirmed a robust ferromagnetic behavior of the nanofluid even at room temperatures. The observed pronounced temperature oscillations of magnetization have been attributed to manifestation of strongly coherent thermo-magnetic response

of the nanofluid (with a hard-sphere type pair correlations between ferromagnetic particles) which could be useful for its potential applications.

Acknowledgments: We acknowledge financial support from the Brazilian agencies CNPq, CAPES, and FAPESP and the Uruguayan agencies CSIC and PEDECIBA.

References and Notes

1. W. Yu and H. Xie, *J. Nanomater.* 2012, 435873 (2012).
2. Y. Ying, E. Gmlke, G. Zhang, and W. Gefei, *J. Nanosci. Nanotechnol.* 5, 571 (2005).
3. H. Zhu, C. Zhang, Y. Tang, J. Wang, B. Ren, and Y. Yin, *Carbon* 45, 226 (2007).
4. J. M. Laskar, J. Philip, and B. Raj, *Phys. Rev. E* 78, 031404 (2008).
5. J. M. Laskar, J. Philip, and B. Raj, *Phys. Rev. E* 80, 041401 (2009).
6. P. D. Shima, J. Philip, and B. Raj, *Appl. Phys. Lett.* 95, 133112 (2009).
7. P. D. Shima, J. Philip, and B. Raj, *Appl. Phys. Lett.* 97, 153113 (2010).
8. J. M. Laskar, J. Philip, and B. Raj, *Phys. Rev. E* 82, 021402 (2010).
9. P. D. Shima, J. Philip, and B. Raj, *J. Phys. Chem. C* 114, 18825 (2010).
10. J. M. Laskar, B. Raj, and J. Philip, *Phys. Rev. E* 84, 051403 (2011).
11. P. D. Shima and J. Philip, *J. Phys. Chem. C* 115, 20097 (2011).
12. V. Mahendran and J. Philip, *Appl. Phys. Lett.* 100, 073104 (2012).
13. E. Tombácz, D. Bica, A. Hajdú, E. Illés, A. Majzik, and L. Vékás, *J. Phys.: Cond. Mat.* 20, 204103 (2008).
14. N. Parkansky, B. Alterkop, R. L. Boxman, G. Leituss, O. Berk, Z. Barkay, Yu. Rosenberg, and N. Eliaz, *Carbon* 46, 215 (2008).
15. M. Jagodic, S. Gyergyek, Z. Jaglicic, D. Makovec, and Z. Trontelj, *J. Appl. Phys.* 104, 074319 (2008).
16. D. Wu, H. Zhu, L. Wang, and L. Liu, *Current Nanosci.* 5, 103 (2009).
17. E. Widenkvist, D. W. Boukhvalov, S. Rubino, S. Akhtar, J. Lu, R. A. Quinlan, M. I. Katsnelson, K. Leifer, H. Grennberg, and U. Jansson, *J. Phys. D* 42, 112003 (2009).
18. M. F. Islam, E. Rojas, D. M. Bergey, A. T. Johnson, and A. G. Yodh, *Nano Lett.* 3, 269 (2003).
19. M. Lotya, P. J. King, U. Khan, S. De, and J. N. Coleman, *ACS Nano* 4, 3155 (2010).
20. R. Asmatulu, A. Fakhari, H. L. Wamocha, H. Y. Chu, Y. Y. Chen, M. M. Eltabey, H. H. Hamdeh, and J. C. Ho, *J. Nanotechnol.* 2009, 238536 (2009).
21. P. K. Prabhakar, S. Vijayaraghavan, J. Philip, and M. Doble, *Current Nanosci.* 7, 371 (2011).
22. C. Alexiou, W. Arnold, P. Hulin, R. J. Klein, H. Renz, F. G. Parak, C. Bergemann, and A. S. Lübke, *J. Magn. Magn. Mater.* 225, 187 (2001).
23. A. S. Lübke, C. Bergemann, H. Riess, F. Schriever, P. Reichardt, K. Possinger, M. Matthias, B. Dörken, F. Herrmann, R. Gürtler, P. Hohenberger, N. Haas, R. Sohr, B. Sander, A.-J. Lemke, D. Ohlendorf, W. Huhnt, and D. Huhn, *Cancer Research* 56, 4686 (1996).
24. A. W. Mombrú, H. Pardo, R. Faccio, O. F. de Lima, A. J. C. Lanfredi, C. A. Cardoso, E. R. Leite, G. Zanelatto, and F. M. Araújo-Moreira, *Phys. Rev. B* 71, 100404 (2005).
25. H. Pardo, R. Faccio, A. W. Mombrú, F. M. Araújo-Moreira, and O. F. de Lima, *Carbon* 44, 565 (2006).
26. S. Sergeenkov, N. S. Souza, C. Speglich, V. A. G. Rivera, C. A. Cardoso, H. Pardo, A. W. Mombrú, and F. M. Araújo-Moreira, *J. Appl. Phys.* 106, 116101 (2009).

27. N. S. Souza, S. Sergeenkov, C. Speglich, V. A. G. Rivera, C. A. Cardoso, H. Pardo, A. W. Mombrú, A. D. Rodrigues, O. F. de Lima, and F. M. Araújo-Moreira, *Appl. Phys. Lett.* 95, 233120 (2009).
28. F. Tuinstra and J. L. Koenig, *J. Chem. Phys.* 53, 1126 (1970).
29. A. S. Dukhin and P. J. Goetz (eds.), *Ultrasound for Characterizing Colloids: Particle Sizing, Zeta Potential and Rheology*, Elsevier, Amsterdam (2002).
30. N. S. Souza, A. D. Rodrigues, C. A. Cardoso, H. Pardo, R. Faccio, A. W. Mombrú, J. C. Galzerani, O. F. de Lima, S. Sergeenkov, and F. M. Araujo-Moreira, *Phys. Lett. A* 376, 544 (2012).
31. H. Xie and L. Chen, *Phys. Lett. A* 373, 1861 (2009).
32. S. Sergeenkov, N. S. Souza, C. Speglich, V. A. G. Rivera, C. A. Cardoso, H. Pardo, A. W. Mombrú, and F. M. Araújo-Moreira, *J. Phys.: Cond. Mat.* 21, 495303 (2009).
33. J. P. Hansen and I. R. McDonald (eds.), *Theory of Simple Liquids*, Academic Press, London (2006).

Delivered by Publishing Technology to: Universidade Federal de Sao Carlos (UFSCAR)
IP: 200.136.245.161 On: Wed, 09 Jan 2013 23:57:55
Copyright American Scientific Publishers